

Autonomous Path Planning Algorithm for Emergency Landing of AAM Considering Wind Disturbances

Hikaru IWAMOTO[1], Nobuhiro YOKOYAMA[2], Takehiro HIGUCHI[1]

[1]Yokohama National University
[2]Japan Aerospace Exploration Agency

Abstract

Advanced Air Mobility (AAM) is expected to play a significant role in future urban and regional transportation. However, emergency landing operations are constrained by multiple factors such as limited battery capacity, wind disturbances, and availability of vertiport resources. In particular, wind can significantly affect energy consumption and reachable landing options, making rapid decision support essential for future m:N operations, i.e., operations of large number of autonomous aircraft by small number of operators. This study proposes a multi-constraint-aware emergency landing decision-support framework that integrates wind-incorporated energy estimation, reachable area analysis, and assessments of vertiport congestion and time-slot allocation feasibility. Candidate vertiports, guidance strategies, and terminal approach profiles are periodically evaluated using a multi-objective cost function based on arrival time, schedule deviation, energy consumption, and congestion level of vertiport. Simulation results show that the proposed method prioritizes early landing in critical cases, while selecting schedule-compatible and congestion-aware solutions in less severe cases. These results indicate that the proposed framework can support safe and operationally feasible emergency landing decision-making under wind disturbances.

Keywords: Advanced Air Mobility, eVTOL, Emergency Decision Support, Reachable Area Analysis, Wind Disturbance

1. Introduction

1.1 Background and Motivation

Advanced Air Mobility (AAM) is expected to provide a new mode of urban and regional transportation by enabling flexible point-to-point mobility. Recent operational concepts emphasize that successful AAM integration requires coordinated development of aircraft, operations, airspace management, infrastructure, and vertiport systems [1]. In particular, practical AAM deployment must account for its unique constraints – such as limited battery capacity, unmatured infrastructure, and dynamic traffic and environmental conditions – while ensuring efficiency and resilience. Furthermore, in future AAM operations, a small number of human operators may supervise large number of aircraft simultaneously. Such m:N multi-vehicle operations [2] are essential for scalable AAM deployment, but they also introduce challenges related to operator workload, situational awareness, and contingency management [2]. These challenges become particularly critical during emergency landing operations, where operators or onboard decision-support systems must rapidly identify a safe and operationally feasible landing option under time and information constraints.

Emergency landing of AAM aircraft is challenging because the available decision margin is affected by limited battery capacity, wind disturbances, and dynamic traffic conditions. During an emergency, reachable alternative vertiports can rapidly decrease as the remaining battery energy decreases. In addition, wind can significantly affect both energy consumption and the reachable area. For example, maintaining a scheduled ground speed under headwind conditions requires a higher airspeed and greater power consumption, whereas tailwind conditions may extend the reachable region. Therefore, emergency landing decisions must consider not only geometric reachability, but also remaining battery margin and wind-aware energy consumption [3]. In addition to these vehicle- and environment-related constraints, infrastructure-related factors must also be incorporated into the decision-making process. Specifically, vertiport availability and congestion must be considered, as part of an integrated decision context, because high-density AAM operations require efficient use of limited takeoff and landing infrastructure while maintaining capacity for emergency aircraft.

Previous studies have addressed scheduling and sequencing of multiple arriving AAM aircraft at vertiports, vertiport approach control, electric aircraft energy management, wind-aware forced landing

and emergency landing guidance [3-6]. Wind and gust conditions can also degrade vertiport airspace traffic performance, indicating the need for wind-dependent scheduling and separation management [7]. However, these topics have often been treated separately, without accounting for their coupled and time-varying effects during emergency situations. Few studies have integrated wind-aware energy estimation, time-reservation feasibility, dynamic vertiport congestion, guidance strategy selection, and terminal approach profile selection into a unified emergency decision-making framework for AAM. Because wind conditions, battery margin, and vertiport availability change over time, and jointly influence feasibility, emergency landing decisions should not be treated as a static, one-time process at the onset of a failure. This motivates a periodic decision framework, in which emergency landing candidates are periodically re-evaluated using the latest aircraft state, remaining battery energy, wind condition, and traffic situation.

1.2 Research Objective

To address the gaps identified in previous literature, the objective of this study is to develop a multi-constraint-aware emergency landing decision-support framework for AAM operations under wind disturbances. The proposed framework assists operators or onboard autonomous systems in selecting an operationally feasible landing option by considering aircraft reachability, remaining battery energy, time-reservation compatibility, vertiport congestion, and the selected decision mode.

To achieve this objective, the proposed method evaluates candidate combinations of landing vertiports, wind-aware guidance strategies, and terminal approach profiles. A multi-objective cost function is formulated to compare feasible candidates by minimizing estimated time to arrival zone entry (ETA), schedule deviation, energy consumption, and vertiport congestion. In addition, these objectives are weighted according to pre-specified decision mode, and a periodic replanning scheme is introduced to adapt the decision-making process to emergency urgency and dynamically changing flight and traffic conditions.

2. Modeling

2.1 Vertiport Network and Time-Reservation Model

The operational environment is modeled to include multiple vertiports, scheduled aircraft, and arrival-time-based reservation slots at each vertiport, which are represented as reservation records. Each reservation record specifies the assigned aircraft, destination vertiport, departure and predicted arrival steps (i.e., discrete time intervals in the planning horizon), and reservation status. In this study, the vertiport capacity represents the number of aircraft that can be accommodated at the vertiport during the corresponding occupancy interval, rather than a detailed model of individual take-off and landing pads or parking stands. The feasibility of an emergency landing candidate is then determined not only by whether the aircraft can physically reach the vertiport, but also by whether the vertiport has available capacity during the predicted occupancy interval.

Let the index set of candidate vertiports be denoted by

$$P = \{p1, p2, \dots, p_{Np}\} \tag{1}$$

where N_p is the number of available vertiports in the operational environment. For each candidate vertiport p, the algorithm evaluates its time-slot feasibility using the ETA of the emergency aircraft. The ETA is denoted by $t_{arr,p}$, and the target arrival time is denoted by $t_{res,p}$. The schedule deviation is then defined as

$$e_{sch,p} = \left| t_{arr,p} - t_{res,p} \right| \tag{2}$$

This term represents the mismatch between the ETA and the reserved time slot. A small schedule deviation indicates that the emergency aircraft can arrive close to the reserved time slot, whereas a large deviation may imply early or late arrival, possibly requiring additional coordination with other traffic. Note that the ETA is defined as the estimated flight time from the emergency trigger to the vertiport arrival zone entry. The schedule error is therefore computed based on this zone-entry time, and the actual flight time until landing completion is generally longer than the ETA due to the terminal approach and descent within the arrival zone.

In addition to the schedule deviation, each vertiport is assigned a congestion-related metric based on its current and future operational state. In the implementation, this metric is computed from the number of currently parked aircraft and future reservations relative to the vertiport capacity. The purpose of this congestion metric is not to model detailed vertiport ground operations, but to provide a compact indicator of whether selecting a given vertiport may increase system-level delay or holding.

This modeling approach allows the emergency landing decision to consider both aircraft-side feasibility and vertiport-side operational feasibility. In other words, a candidate vertiport is evaluated not only as a reachable landing site, but also as a time-compatible and congestion-aware landing option.

2.2 Aircraft Dynamics, Power Consumption, and Wind-Aware Guidance Model

To accurately and quickly estimate the reachable range and energy consumption under wind disturbances, the AAM aircraft is modeled as a point-mass with three degrees of freedom. The equations of motion describe the translational dynamics in horizontal and vertical directions as well as the heading dynamics of the vehicle as follows:

$$\begin{aligned} \dot{x} &= U\cos\psi + \omega_x \\ \dot{y} &= U\sin\psi + \omega_y \\ \dot{h} &= W + \omega_h \end{aligned} \tag{3}$$

$$\begin{aligned} \dot{U} &= -\frac{T\sin\theta\cos\phi + D\cos\gamma}{m} \\ \dot{W} &= \frac{T\cos\theta\cos\phi - D\sin\gamma}{m} - g \\ \dot{\psi} &= \frac{T\cos(\theta-\gamma)\sin\phi}{mU} \end{aligned} \tag{4}$$

where x and y denote the horizontal position in the local-level frame, and h denotes the altitude. U and W are the horizontal and vertical components of the airspeed, respectively, ψ is the heading angle of the airspeed vector, T represents the total thrust generated by the propulsion system, ϕ and θ are the roll and pitch angles of the thrust vector, m is the vehicle mass, and g is the gravitational acceleration. The model is assumed as multicopter and it explicitly accounts for thrust forces, aerodynamic drag, and gravitational acceleration. As expressed in (3), wind effects are additive disturbances to the airspeed, enabling a consistent representation of the coupled evolution of position, velocity, and heading under realistic atmospheric conditions.

The energy consumption rate $\dot{Q}$ is expressed as the sum of three aerodynamic components adjusted by the *total* efficiency η_{total}, i.e.,

$$\dot{Q} = \frac{1}{\eta_{total}}\left(P_{prof} + P_{ind} + P_{clim}\right) \tag{5}$$

Here, P_{prof} (profile power) accounts for the power required to overcome aerodynamic drag on the rotor blades, which increases significantly with forward speed and wind turbulence, P_{ind} (induced power) represents the power required to generate lift, and P_{clim} (climb power) corresponds to the power done against gravity. This formulation allows the system to quantify the energy penalty caused by headwinds, providing the following estimation:

$$E_{k+1} = E_k - \dot{Q}_k \Delta t \tag{6}$$

where E_k is the remaining battery energy at time step k, $\dot{Q}_k$ is the estimated power consumption at that step, and Δt is the simulation time step. This estimation is used to evaluate whether each candidate vertiport can be reached while maintaining the required energy margin.

In the time-domain simulation, the guidance module generates reference commands for speed, altitude, and ground-track angle, rather than directly prescribing the control inputs. These commands are first converted into air-relative speed and heading commands by considering the local wind velocity. An inverse-model-based tracking controller then computes the thrust T, pitch angle θ, and roll angleϕ so that the aircraft follows the commanded trajectory under the point-mass dynamics. The resulting state trajectory and power consumption are used for candidate evaluation and battery-energy updating.

Based on the relationship between airspeed, ground speed, and windspeed, two wind-aware guidance strategies are defined. Strategy A is a ground-speed command strategy, where the aircraft commands a desired ground speed along the route to the selected vertiport. This strategy is suitable for four-dimensional operation because the arrival time can be controlled more directly. However, under headwind conditions, maintaining the commanded ground speed requires a larger airspeed,

which may increase power consumption and reduce the reachable area. Strategy B is an airspeed-based strategy. In this mode, the aircraft maintains a prescribed airspeed while flying toward the selected vertiport. This strategy can reduce energy consumption and extend reachability under adverse wind conditions. However, the resulting ground speed depends on the wind condition, and therefore the arrival time may deviate from the reserved or target arrival time.

These two strategies represent a trade-off between schedule adherence and energy-aware reachability. Strategy A prioritizes time-of-arrival control by regulating the ground speed, whereas Strategy B prioritizes energy feasibility by regulating the airspeed. The proposed decision framework evaluates both strategies as candidate guidance modes for each vertiport and selects the most suitable option according to the multi-objective cost and decision-mode weighting.

To clarify the difference between the two strategies, a preliminary reachable-area comparison was conducted under a 15 m/s headwind condition. In this comparison, the nominal command speed was set to 30 m/s.

In Strategy A, this value is interpreted as the commanded ground speed. Therefore, under a pure 15 m/s headwind, the aircraft must fly at an airspeed of approximately 45 m/s to maintain the 30 m/s ground-speed command. In the route-dependent simulation, the required airspeed reached up to 42.8 m/s, exceeding the aircraft airspeed limit of 30.9 m/s. Thus, Strategy A can become infeasible under strong headwind conditions.

In Strategy B, the same 30 m/s value is interpreted as the commanded airspeed. Therefore, the airspeed remains within the aircraft limit, while the resulting ground speed decreases according to the headwind component. For a pure 15 m/s headwind, the resulting ground speed becomes approximately 15 m/s. This improves reachability and energy feasibility, but makes the arrival time more sensitive to wind.

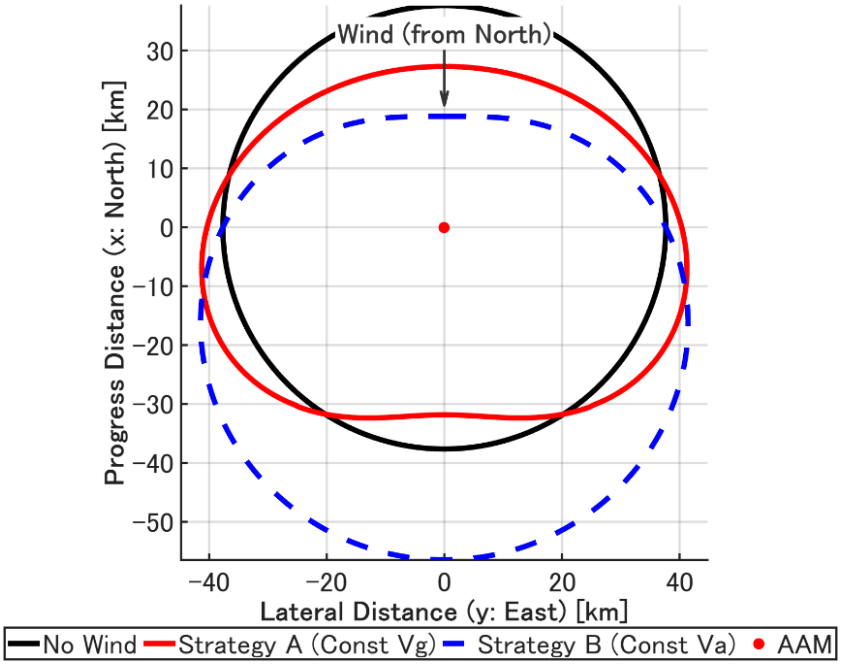


Figure 1 – AAM reachability comparison (Strategy A vs Strategy B) under 15 m/s wind.

Figure 1 compares the reachable areas obtained using Strategy A and Strategy B under the 15 m/s headwind condition. This figure is used as a preliminary illustration of the wind-aware guidance model rather than as a main simulation result.

Strategy A provides better compatibility with schedule-oriented operation when the required airspeed remains within the aircraft limit. However, under strong headwind conditions, the increased airspeed demand reduces the reachable region. In contrast, Strategy B preserves a larger reachable region by directly limiting the commanded airspeed, although the resulting ground speed and arrival time vary with the wind condition.

This comparison illustrates why both strategies are included in the proposed decision framework. Strategy A is useful for arrival-time control when wind conditions are moderate, whereas Strategy B provides a more robust fallback option when headwind conditions make the ground-speed command infeasible.

2.3 Terminal Approach Profile Model

In addition to the cruise guidance strategy defined above, the terminal approach phase is also modeled as a discrete decision component. In emergency landing operations, the terminal phase affects not only the final arrival time, but also the energy consumption and the occupancy time of the vertiport airspace. Therefore, three predefined terminal approach profiles are introduced: STEEP, NOMINAL, and SHALLOW. Each approach profile is characterized by the approach radius, the minimum approach speed, and the vertical landing descent rate. The approach radius defines the distance from the selected vertiport at which the aircraft transitions from the cruise phase to the terminal approach phase. The minimum approach speed determines the lower bound of the horizontal speed near the vertiport. The landing descent rate determines the vertical descent speed during the final landing phase.

The three terminal approach profiles used in this study are summarized in Table 1.

Table 1. Terminal approach profiles.

Profile Name	Approach Radius (Rapp) [m]	Min. Approach Speed (Vmin) [m/s]	Landing Descent Rate (Wland) [m/s]
STEEP	700	4.0	2.5
NOMINAL	1000	5.0	2.0
SHALLOW	1500	7.0	1.5

The STEEP profile uses a shorter approach radius and a higher descent rate. This profile tends to reduce the terminal approach time, but it requires a more aggressive terminal maneuver. The SHALLOW profile uses a larger approach radius and a lower descent rate. This profile provides a more gradual terminal approach, but it may increase the time spent in the terminal airspace. The NOMINAL profile is defined as an intermediate profile between these two cases.

During the terminal approach phase, the horizontal speed command is gradually reduced as the aircraft approaches the selected vertiport. Let d be the horizontal distance from the aircraft to the selected vertiport, R_{app} be the approach radius, V_{cruise} be the cruise speed, and $V_{app,min}$ be the minimum approach speed. The commanded approach speed is given by

$$V_{app}(d) = V_{app,min} + \left(V_{cruise} - V_{app,min} \right) \times \min\left(\frac{d}{R_{app}}, 1 \right) \tag{7}$$

The altitude command is also reduced according to the distance to the vertiport. In this study, a linear altitude profile is used:

$$h_{cmd}(d) = h_{cruise,min} \times \min\left(\frac{d}{R_{app}}, 1 \right) \tag{8}$$

where h_{cruise} is the cruise altitude. When the aircraft reaches the vicinity of the vertiport, it transitions to the vertical landing phase and descends with the specified landing descent rate.

In the proposed decision framework, the terminal approach profile is evaluated together with the candidate vertiport and guidance strategy. This allows the terminal-phase time and energy characteristics to be reflected in the emergency landing decision.

3. Proposed Emergency Decision Algorithm

This section describes the proposed emergency landing decision algorithm. The objective of the algorithm is to select an operationally feasible landing option by considering aircraft reachability, remaining battery energy, time-reservation compatibility, and vertiport congestion. The algorithm evaluates combinations of candidate vertiports, wind-aware guidance strategies, and terminal approach profiles.

The proposed algorithm consists of three main steps: candidate generation, feasibility evaluation, and multi-objective cost evaluation. First, emergency landing candidates are generated by combining vertiports, guidance strategies, and terminal approach profiles. Second, each candidate is checked for reachability, battery margin, and time-reservation availability. Third, feasible candidates are

compared using a multi-objective cost function based on estimated arrival time, schedule deviation, energy consumption, and vertiport congestion.

The weighting coefficients in the cost function are specified in advance according to the selected decision mode or operator preference. The algorithm does not automatically determine emergency severity or change the decision mode during flight. During the diversion flight, the above three-step process is repeated periodically using the latest aircraft state, remaining battery energy, wind condition, and vertiport occupancy.

3.1 Candidate Generation

At the time of an emergency, the algorithm first generates a set of candidate emergency landing options. Let $P_c \subseteq P$ denote the set of candidate vertiports located within a predefined search radius from the current position of the emergency aircraft. In the present simulation, this search condition can be set to include all vertiports, whereas the formulation allows the search space to be restricted by a finite radius. The candidate vertiports are selected based on the current aircraft state and the search condition used in the decision module.

Each emergency landing candidate is defined as a combination of a candidate vertiport, a wind-aware guidance strategy, and a terminal approach profile. Let C denote the set of guidance strategies and A denote the set of terminal approach profiles. The candidate set C is defined as

$$C = \{c = (p, s, a) | p \in P_c, s \in S, a \in A\} \tag{9}$$

In this study, the guidance strategy set is defined as

$$S = \{Strategy\ A, Strategy\ B\} \tag{10}$$

where Strategy A represents the ground-speed command strategy and Strategy B represents the airspeed-based strategy. The terminal approach profile set is defined as

$$A = \{STEEP, NOMINAL, SHALLOW\} \tag{11}$$

For each candidate $c = (p, s, a)$, the algorithm performs a fast time-domain simulation from the current emergency state to the selected vertiport using the aircraft dynamics, control, and power-consumption model described in Section 2. Through this simulation, the algorithm estimates the arrival time, flight time, energy consumption, remaining battery energy, schedule deviation, and congestion-related information for each candidate. The feasibility and cost evaluation are described in the following subsections.

3.2 Feasibility Evaluation

After candidate generation, each candidate is evaluated for feasibility. A candidate is regarded as feasible if the simulated trajectory reaches the selected vertiport within the evaluation horizon, the predicted energy consumption satisfies the required battery margin, and the selected vertiport has available capacity.

Reachability and energy feasibility are evaluated from the time-domain simulation results obtained for each candidate. In the implementation, the candidate is feasible only when the aircraft arrives at the selected vertiport and both the cruise-phase and total energy constraints are satisfied. The battery feasibility conditions are expressed as

$$\begin{aligned} Q_{cruise,c} &\leq Q_{remain} - Q_{land,res} \\ Q_{total,c} &\leq Q_{remain} - Q_{post,res} \end{aligned} \tag{12}$$

where $Q_{cruise,c}$ and $Q_{total,c}$ are the cruise-phase and total energy consumption of candidate c, Q_{remain} is the remaining battery energy at the decision time, $Q_{land,res}$ is the energy reserved for terminal approach and landing, and $Q_{post,res}$ is the required post-landing reserve.

Vertiport capacity is checked using the current parked aircraft count and the capacity of the selected vertiport. If the selected vertiport is already full, the candidate is marked as infeasible.

3.3 Multi-Objective Cost Evaluation

After the feasibility evaluation, the feasible candidates are compared using a multi-objective cost function. The purpose of this evaluation process is to select an emergency landing option that balances aircraft-side safety and system-level operational stability.

Let C_f denote the set of feasible candidates at the current decision step. For each feasible candidate $c \in C_f$, the total cost $J(c)$ is defined as

$$J(c) = w_{ETA}\hat{J}_{ETA}(c) + w_{sch}\hat{J}_{sch}(c) + w_E\hat{J}_E(c) + w_{cong}\hat{J}_{cong}(c) \quad (13)$$

Here, $\hat{J}_{ETA}(c), \hat{J}_{sch}(c), \hat{J}_E(c), \hat{J}_{cong}(c)$ denote the normalized ETA, schedule deviation, energy consumption, and vertiport congestion, respectively. The corresponding weights are denoted by w_{ETA}, w_{sch}, w_E, and w_{cong}.

The ETA term represents the urgency of the emergency landing. It penalizes candidates with longer estimated flight time to the arrival zone and therefore promotes rapid landing. A larger w_{ETA}, makes the decision more time-critical.

The schedule-deviation term represents compatibility with the reserved arrival time. It penalizes candidates that arrive too early or too late relative to the target reservation time. A larger w_{sch} makes the decision more schedule-oriented.

The energy term represents battery preservation. It penalizes candidates with larger predicted energy consumption and therefore encourages the selection of energy-efficient options. A larger w_E makes the decision more conservative with respect to remaining battery energy.

The congestion term represents the load level of the selected vertiport. In this study, the vertiport congestion metric is computed from the number of currently parked aircraft and future reservations relative to the vertiport capacity. Therefore, a larger congestion value indicates that the vertiport is already heavily loaded and that selecting it may increase the risk of ground delay or landing hold for other aircraft. A larger w_{cong} penalizes such highly loaded vertiports and encourages the selection of less congested alternatives when they are reachable and feasible.

Each evaluation metric is normalized among the feasible candidates at the current decision step. For a generic metric $J_n(c)$, the normalized value is computed as

$$\hat{J}_k(c) = \frac{J_n(c) - J_n^{min}}{J_n^{max} - J_n^{min}} \quad (14)$$

where J_n^{min} and J_n^{max} are the minimum and maximum values of metric n among the feasible candidates. When all feasible candidates have the same value for a metric, the normalized value of that metric is set to zero for numerical stability.

The selected emergency landing option c^* is obtained by minimizing the total cost:

$$c^* = arg\min_{c \in C_f} J(c) \quad (15)$$

Since each normalized metric is formulated such that smaller values are preferable, a lower total cost indicates a more desirable emergency landing candidate.

By combining these normalized terms, the proposed cost function evaluates metrics with different physical units in a unified framework. The ETA and energy terms represent aircraft-side urgency and battery feasibility, whereas the schedule deviation and congestion terms represent compatibility with planned traffic flow and vertiport operations. Therefore, the proposed cost provides a balanced criterion for selecting a landing vertiport, guidance strategy, and terminal approach profile while considering both individual aircraft safety and system-level operational stability.

3.4 Decision-Mode Weighting

The relative importance of the evaluation metrics depends on the operational priority specified by the selected decision mode. In a time-critical situation, the aircraft should prioritize rapid landing and energy feasibility, even if the selected option causes schedule deviation or additional congestion. In contrast, when sufficient time and energy margin remain, the decision can place greater emphasis on schedule compatibility and traffic stability.

To represent these different operational priorities, decision-mode weighting is introduced in the multi-objective cost function. In this study, the weighting coefficients are specified in advance according to the selected decision mode or operator preference. The algorithm does not automatically determine the decision mode during flight; instead, the same candidate generation and feasibility evaluation process is used while only the objective weights are changed.

The specific weighting parameters used in the numerical simulations are provided in Section 4.

3.5 Periodic Replanning

The emergency landing decision is not treated as a one-time process. During the diversion flight, atmospheric conditions, remaining battery energy, and vertiport availability may change over time. Therefore, the proposed algorithm periodically updates the emergency landing decision by re-evaluating the candidate set using the latest operational state.

Let Δt_{plan} denote the replanning interval. At each replanning time, the current aircraft state, remaining battery energy, wind condition, and vertiport occupancy status are updated. The algorithm then regenerates the candidate set within the search radius and repeats the feasibility evaluation, multi-objective cost evaluation, and decision-mode-based selection process described in the previous subsections. In the implementation used in this study, the selected option is updated only when a newly evaluated candidate provides sufficient improvement in the multi-objective cost, in order to avoid frequent switching caused by small cost differences. The selected candidate at replanning step *n* is given by

$$c_n^* = arg\min_{c \in C_f} J(c), c \in C_f(t_n) \tag{16}$$

ere $C_f(t_n)$ is the feasible candidate set at replanning time t_n, and $J_n(c)$ is the multi-objective cost computed using the updated state information.

This periodic replanning enables the decision system to adapt to changes during the emergency operation. If an unexpected headwind increases energy consumption, the algorithm may select a closer vertiport or switch to a more energy-efficient guidance strategy, such as Strategy B. If the previously selected vertiport becomes less suitable due to changes in occupancy or traffic delay, the algorithm can select an alternative vertiport with better capacity or time-reservation compatibility. In addition, as the aircraft approaches the terminal area, the selected terminal approach profile can be updated to reduce schedule deviation relative to the reserved arrival time.

By repeatedly updating the decision, the proposed framework maintains feasibility with respect to reachability, battery margin, and vertiport availability throughout the diversion flight. This allows the emergency landing plan to adapt from the initial diversion decision to the final terminal approach while balancing individual aircraft safety and system-level operational stability.

3.6 Replanning Effect

As described above, the emergency landing decision was updated periodically during the diversion flight using a replanning process. This process allows the decision module to monitor whether the currently selected option remains feasible and operationally suitable until the final landing phase.

However, excessively frequent replanning may cause repeated switching of the selected guidance strategy or terminal approach profile before the aircraft response has sufficiently settled. Such behavior can lead to chattering-like transients in speed, attitude, and thrust commands. Therefore, the replanning interval was selected by considering not only decision responsiveness, but also the settling behavior of the aircraft after mode switching.

To evaluate this effect, a switching-interval test was conducted. The settling ratio was defined as the ratio between the residual error at the end of a switching interval and the initial error immediately after the switch. A smaller value indicates that the aircraft response sufficiently converged before the next switching event. In this study, a settling ratio below 0.3 was regarded as sufficiently settled.

Table 2. Switching-interval evaluation for replanning stability.

Switching interval [s]	Number of switches	Not-settled intervals	Average settling ratio
1	620	311	0.971
2	309	155	0.919
5	122	62	0.794
10	60	31	0.649
30	19	11	0.347
60	9	1	0.124
80	6	0	0.009

As shown in Table 2, short switching intervals resulted in many not-settled intervals. For example, the average settling ratio was 0.971 for a 1 s interval and 0.794 for a 5 s interval, indicating that the aircraft response did not sufficiently converge before the next switching event. In contrast, the average settling ratio decreased to 0.124 for a 60 s interval and 0.009 for an 80 s interval. These results indicate that

a replanning interval on the order of 60–80 s is sufficient to avoid excessive switching transients.

Based on this result, the replanning interval in the main traffic simulation was set to 70 s, as described in 4.1. This value provides a compromise between decision responsiveness and switching stability. In the 10 m/s wind case, the periodic replanning process enabled the system to re-evaluate the selected vertiport and approach profile while maintaining a stable decision trend. Therefore, the periodic replanning framework contributes not only to feasibility monitoring, but also to stable emergency decision-making without unnecessary frequent switching.

4. Simulation Results

4.1 Simulation Setup

To evaluate the proposed framework, a high-density AAM traffic simulation was conducted using 23 aircraft, consisting of one emergency aircraft and 22 background traffic aircraft, and 13 vertiports, as shown in Fig. 2. The background aircraft followed pre-planned time-reservation-based operations, while the emergency aircraft was required to select an alternative landing option after the emergency trigger.

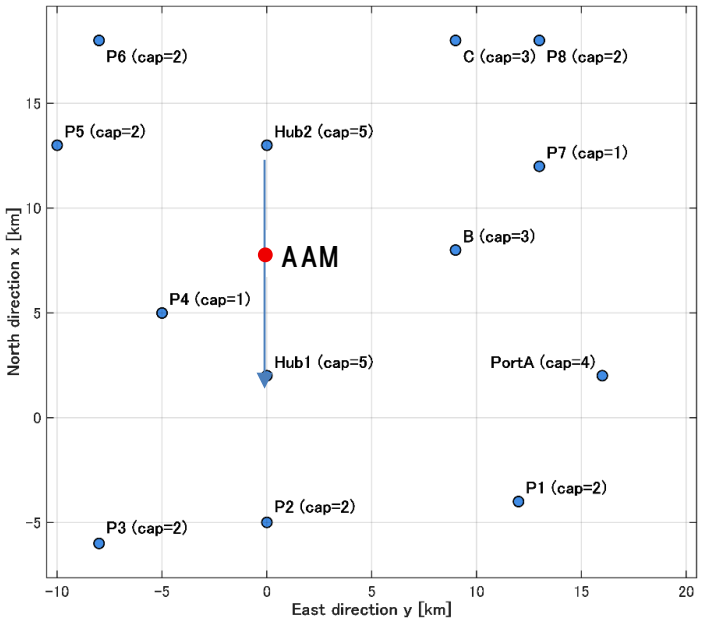


Figure 2. Vertiport layout and capacity used in the simulation

Figure 2 shows the spatial distribution and capacity of the vertiports used in the simulation.

The value in parentheses indicates the capacity of each vertiport. Hub1 and Hub2 were modeled as major vertiports with a capacity of five aircraft, while the other vertiports were assigned to smaller capacities according to their assumed operational scale.

The simulation time step was set to 5 s. The aircraft cruise speed was set to 54 kt, which corresponds to approximately 27.8 m/s. Two constant wind conditions, 15 m/s and 10 m/s, were considered to evaluate the proposed decision logic under strong and moderate wind disturbances. In the local coordinate frame, the wind vector was set as (15.0,0.0) m/s or (10.0,0.0) m/s.

The emergency aircraft was originally operating on a route from Hub2 to Hub1. The emergency was triggered at 1235 s after the start of the simulation, while the aircraft was in cruise flight at an altitude of approximately 427 m between the two vertiports. The pre-planned arrival time, representing the original time reservation of the emergency aircraft, was set to 320 s after the trigger. Periodic replanning was performed every 70 s. This interval was selected to balance computational efficiency with the ability to adaptively update the diversion plan based on the aircraft state, remaining battery energy, wind condition, and vertiport occupancy.

The weighting parameters used in the simulations are summarized in Table 3. Four decision modes were evaluated to examine the effect of each objective term in the cost function. Because ETA and schedule deviation represent conflicting operational priorities, the schedule deviation weight is set to zero in the Time-Critical mode, whereas the ETA weight is set to zero in the Schedule-Oriented mode. The Energy-Saving and Congestion-Aware modes emphasize battery consumption and vertiport congestion, respectively, while retaining a small ETA weight to avoid excessively delayed landing

decisions.

Table 3. Weighting parameters for decision modes

Decision modes	w_{ETA}	w_{sch}	w_E	w_{cong}
Time-Critical	0.7	0.0	0.2	0.1
Schedule-Oriented	0.0	0.7	0.2	0.1
Energy-Saving	0.1	0.0	0.8	0.1
Congestion-Aware	0.1	0.0	0.2	0.7

4.2 Decision results under 15 m/s wind

To evaluate the decision behavior under a strong wind condition, the proposed framework was first applied to the 15 m/s wind case. As mentioned previously, the ground-speed-based Strategy A becomes more restrictive under strong headwind conditions because maintaining the commanded ground speed requires a higher airspeed and larger power consumption. Therefore, the strong-wind case is used to examine whether the proposed decision module can select an operationally feasible fallback strategy when schedule-oriented ground-speed operation becomes difficult.

Table 4 summarizes the selected emergency landing options for the four decision modes under the 15 m/s wind condition. The schedule error is computed from the predicted arrival time used in the candidate evaluation, whereas the flight time represents the actual time until landing completion in the time-domain simulation.

Table 4. Selected emergency landing options under 15 m/s wind.

Decision mode	Time-Critical	Schedule-Oriented	Energy-Saving	Congestion-Aware
Selected vertiport	Hub2	Hub2	Hub2	Hub2
Strategy	B	B→A	B	B
Approach profile	STEEP	NOMINAL	STEEP	STEEP
ETA (flight time to arrival zone) [s]	305	320	305	305
Schedule error [s]	15	0	15	15
Flight time[s]	180	335	180	180
Battery at landing [kWh]	20.47	15.03	20.47	20.47

At the initial decision step, all decision modes selected Hub2 with Strategy B as the initial guidance strategy. Strategy A was infeasible for most vertiports because maintaining the commanded ground speed against the 15 m/s headwind required an airspeed of up to 42.8 m/s, exceeding the aircraft airspeed limit of 30.9 m/s. Even for Hub2, where Strategy A remained feasible at the initial step, Strategy A consumed 8.01 kWh and produced a schedule error of 85 s, whereas Strategy B consumed 5.79 kWh and produced a schedule error of 15 s. Therefore, Strategy B was selected as the more feasible initial guidance option under the strong wind condition.

Although all four modes selected Hub2 with Strategy B at the initial decision step, the selected terminal approach profile differed depending on the decision-mode weighting. The Time-Critical, Energy-Saving, and Congestion-Aware modes selected the STEEP profile. This profile resulted in the shortest

flight time of 180 s and the highest remaining battery energy of 20.47 kWh among the selected results. In these three modes, reducing flight time and energy consumption was more important than precise schedule matching, and therefore the STEEP profile became the most favorable option.

In contrast, the Schedule-Oriented mode selected the NOMINAL profile and later switched the guidance strategy from Strategy B to Strategy A during replanning. The final estimated arrival time became 320 s after the emergency trigger, which exactly matched the target reservation time and resulted in zero schedule error. However, this improvement in schedule compatibility required a longer flight time of 335 s and reduced the remaining battery energy to 15.03 kWh. This result shows that the Schedule-Oriented mode sacrificed flight time and battery margin in order to improve arrival-time compatibility.

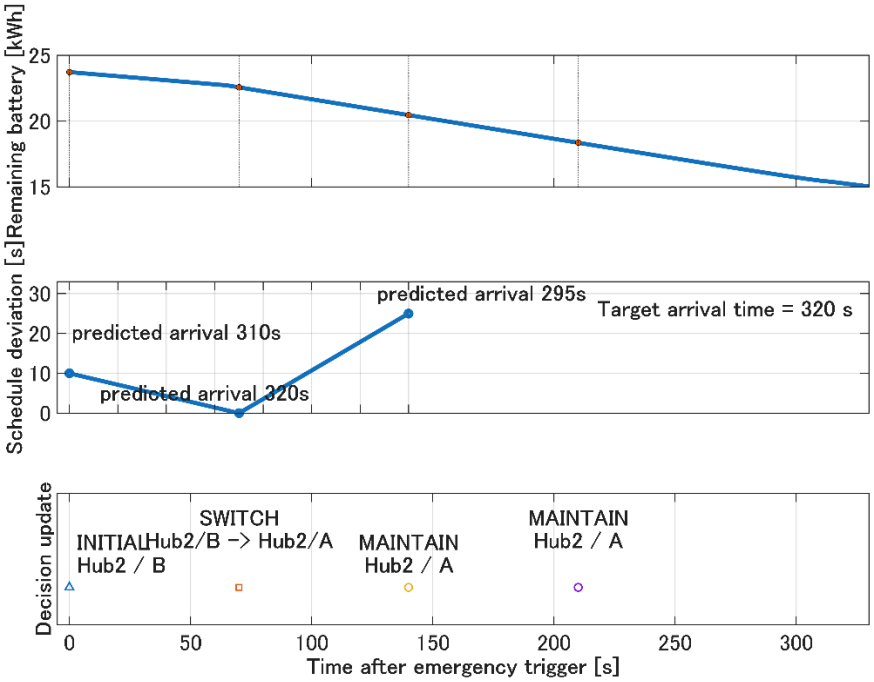


Figure 3. Replanning timeline for the Schedule-Oriented mode under 15 m/s wind

Figure 3 shows the replanning timeline for the Schedule-Oriented mode under the 15 m/s wind condition. At the initial step, the aircraft selected Hub2 with Strategy B because Strategy B provided better energy feasibility under the strong headwind. At t=70 s, the selected guidance strategy switched from Strategy B to Strategy A. This switch became feasible because the aircraft had approached Hub2 and the required airspeed for ground-speed-based control dropped below the aircraft limit. As a result, Strategy A was able to provide more accurate arrival-time control near the destination, and the final schedule error was reduced to 0 s.

The Congestion-Aware mode also selected Hub2 with Strategy B and the STEEP profile. Although this mode assigned a high weight to vertiport congestion, Hub2 was the only energetically reachable vertiport under the 15 m/s condition. Therefore, the congestion term could not lead to the selection of an alternative vertiport. This result illustrates an important boundary condition of the proposed framework: congestion-aware weighting becomes effective only when multiple feasible vertiports with different congestion levels are available. When the feasible set is restricted by wind and battery constraints, the decision is dominated by reachability and energy feasibility.

Overall, the 15 m/s wind case demonstrates the fallback capability of the proposed framework under strong wind and limited reachability conditions. The decision module automatically selected the airspeed-based Strategy B because the ground-speed-based Strategy A was strongly constrained by the airspeed limit under the 15 m/s headwind. In addition, the Schedule-Oriented mode was able to refine the guidance strategy to Strategy A during replanning once the airspeed constraint became less restrictive. These results indicate that the proposed framework can adapt both the guidance strategy and the terminal approach profile according to wind-dependent feasibility and decision-mode weighting.

4.3 Decision-mode comparison under 10 m/s wind

To further examine the effect of decision-mode weighting under a moderate wind condition, the proposed framework was applied to the 10 m/s wind case. Compared with the 15 m/s case, the feasible candidate set became less restrictive, and multiple vertiport, guidance-strategy, and terminal-approach combinations remained available. Therefore, this case is used to evaluate whether the proposed multi-objective cost can change the selected emergency landing option according to the operational priority.

Under the 10 m/s wind condition, the feasible candidate set expanded to 11 combinations out of 78 evaluated combinations. Unlike the 15 m/s case, Strategy A was feasible for several nearby vertiports, including P4 and Hub2. This indicates that the feasibility of the ground-speed-based strategy is sensitive to both wind speed and vertiport geometry. Therefore, evaluating both Strategy A and Strategy B is important for maintaining feasible options under wind disturbances.

Table 5 summarizes the selected emergency landing options for the four decision modes under the 10 m/s wind condition.

Table 5. Selected emergency landing options under 10 m/s wind

Decision mode	Time-Critical	Schedule-Oriented	Energy-Saving	Congestion-Aware
Selected vertiport	Hub2	Hub2	Hub2	P4
Strategy	B	B→A	B	B
Approach profile	STEEP	NOMINAL*	STEEP	SHALLOW
ETA (flight time to arrival zone) [s]	255	340	255	345
Schedule error [s]	65	20	65	25
Flight time[s]	195	345	195	310
Battery at landing [kWh]	20.23	16.75	20.23	18.67

* In the Schedule-Oriented case, the selected terminal approach profile had a close cost relationship with the alternative profile at the final replanning step. Therefore, the discussion focuses mainly on the selected vertiport and guidance-strategy transition.

The Time-Critical and Energy-Saving modes selected Hub2 with Strategy B and the STEEP approach profile. This option provided the shortest flight time of 195 s and the highest remaining battery energy of 20.23 kWh among the selected results. However, the predicted arrival time was 255 s, which was 65 s earlier than the target arrival time of 320 s. These results indicate that the Time-Critical and Energy-Saving modes prioritized rapid and energy-efficient landing over schedule compatibility.

The Schedule-Oriented mode exhibited a more dynamic replanning behavior. Although the initial decision selected P4 with Strategy A because it provided a small schedule error, the selected option changed during the diversion flight as the aircraft state, battery energy, candidate feasibility, and candidate cost were updated.

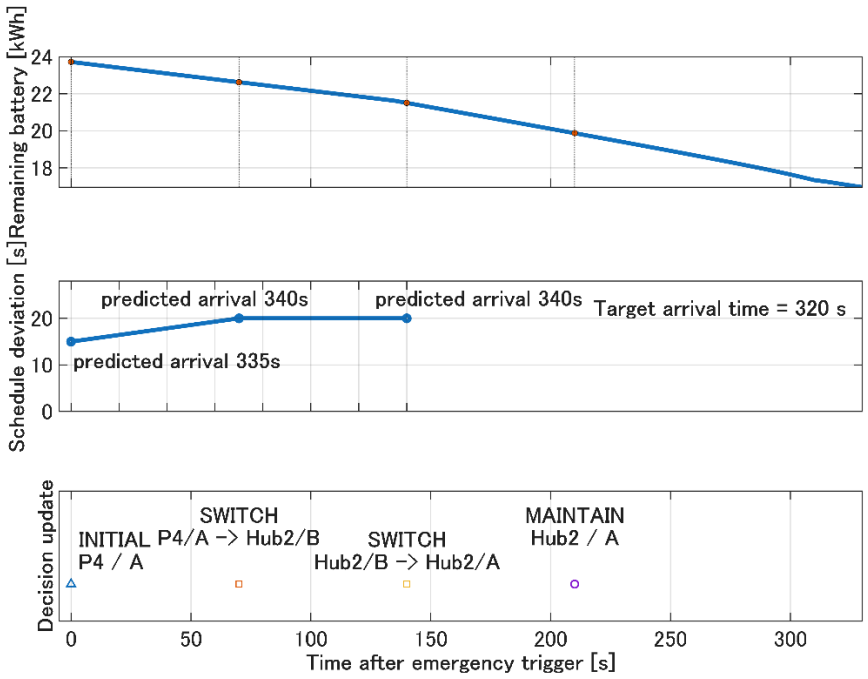


Figure 4. Replanning timeline for the Schedule-Oriented mode under 10 m/s wind

Figure 4 shows the replanning timeline for the Schedule-Oriented mode. At t=0 s, the system selected P4 with Strategy A because it provided a predicted arrival time of 335 s, corresponding to a schedule error of 15 s relative to the target reservation time of 320 s. At t=70 s, the decision switched from P4/Strategy A to Hub2/Strategy B. This switch occurred because Hub2/Strategy B produced a predicted arrival time of 340 s, corresponding to a schedule error of 20 s, whereas the P4/Strategy A candidate produced a larger schedule error of 35 s at the same replanning step. In addition, Hub2/Strategy B had a lower predicted energy consumption than the P4/Strategy A candidate. Therefore, Hub2/Strategy B became the lower-cost option under the schedule-oriented weighting.

At t=140 s, the decision switched again from Hub2/Strategy B to Hub2/Strategy A. At this replanning step, the P4 candidates were no longer feasible because the cruise-energy reserve constraint was violated, not because of vertiport capacity saturation. P4 had no current occupancy or conflicting future reservation at this step; however, the remaining battery margin was insufficient to satisfy the required landing reserve for the P4 candidates. Therefore, the decision remained at Hub2, and Strategy A became the lower-cost option for Hub2. At t=210 s, the selected Hub2/Strategy A option was maintained. The final predicted arrival time was 340 s, corresponding to a schedule error of 20 s, with a flight time of 345 s and a remaining battery energy of 16.75 kWh.

This behavior shows that the Schedule-Oriented mode does not simply maintain the initially selected vertiport. Instead, it updates the selected vertiport and guidance strategy according to the latest schedule feasibility, energy margin, and candidate cost. In this scenario, the initially selected P4 option was favorable at the beginning because of its schedule compatibility. However, as the aircraft state and energy margin changed during replanning, Hub2 became the lower-cost schedule-compatible option. As a result, the Schedule-Oriented mode eventually selected Hub2, the same vertiport selected by the Time-Critical and Energy-Saving modes.

In contrast, the Congestion-Aware mode selected P4 with Strategy B and maintained this option throughout the diversion flight.

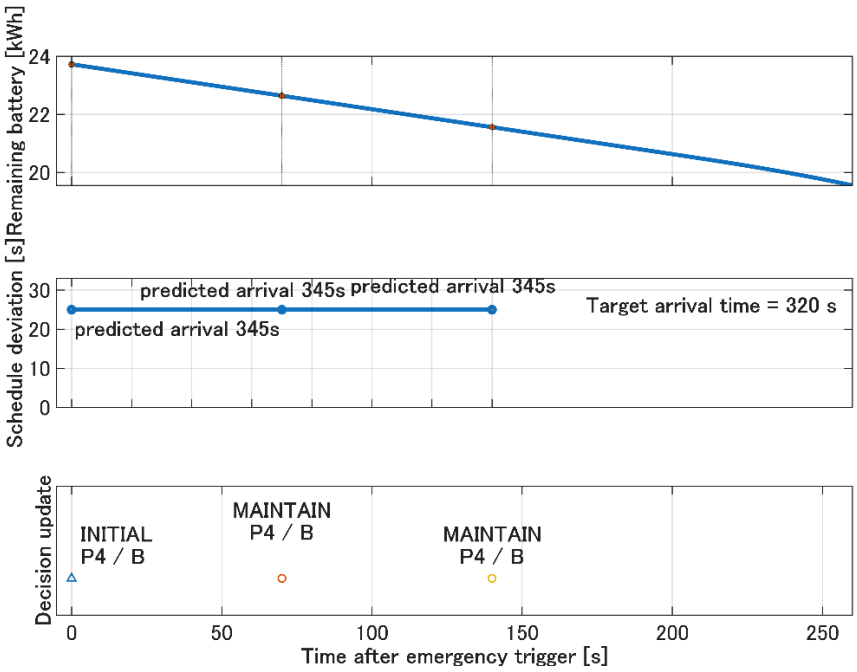


Figure 5. Replanning timeline for the Congestion-Aware mode under 10 m/s wind

Figure 5 shows the replanning timeline for the Congestion-Aware mode. Unlike the Schedule-Oriented mode, the selected option remained P4 with Strategy B at all replanning steps. The predicted arrival time remained 345 s, and the schedule error remained 25 s. Although this option required a longer individual flight than the Hub2 solution, it avoided selecting the highly loaded Hub2. This stable decision history indicates that the congestion term consistently favored the low-load vertiport when multiple feasible options were available.

The reason for this stable P4 selection can be understood from the vertiport congestion state.

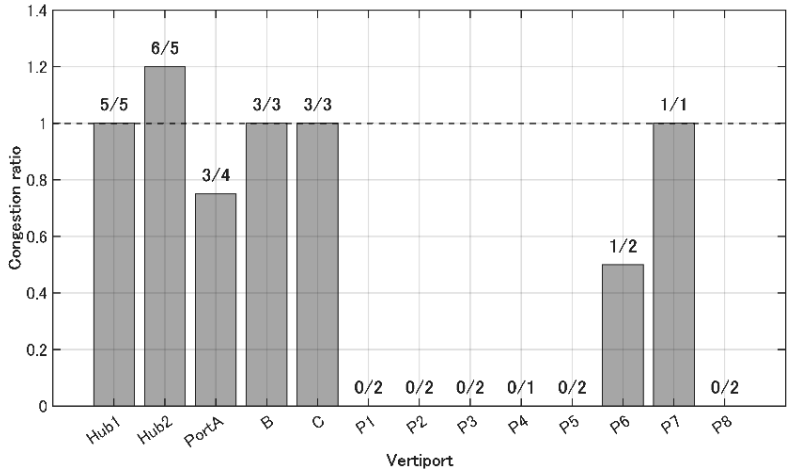


Figure 6. Vertiport congestion ratio at the initial decision step under 10 m/s wind

Figure 6 shows the vertiport congestion ratio at the initial decision step. Hub2 had a congestion ratio of 1.20, with 6 occupied or reserved aircraft against a capacity of 5. Note that the congestion ratio may exceed 1.0 when future reservations span different time windows; this does not indicate a simultaneous capacity violation, but reflects a high scheduling load that may increase system-level delays. In contrast, P4 had no current occupancy or conflicting reservation, resulting in a congestion ratio of 0.00. Therefore, the congestion term strongly penalized Hub2 and made P4 more favorable in the Congestion-Aware mode. This result demonstrates that the proposed congestion-aware weighting can change the selected vertiport when multiple energetically reachable options are available. Another informative feature of the Congestion-Aware result is the selection of the SHALLOW approach profile at P4.

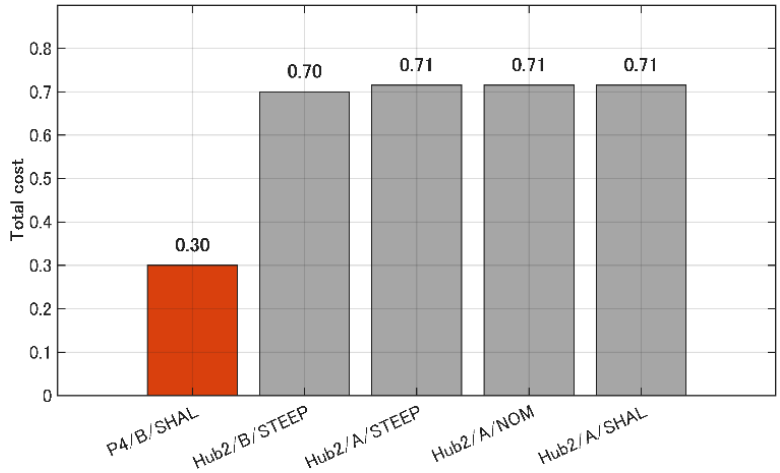


Figure 7. Profile-level tradeoff for P4/Strategy B in the Congestion-Aware mode under 10 m/s wind

Figure 7 shows the tradeoff among terminal approach profiles for P4 with Strategy B. The STEEP and NOMINAL profiles consumed less energy, but they produced much earlier predicted arrival times relative to the target reservation time. The SHALLOW profile consumed more energy but produced a predicted arrival time closer to the target time. Even though the schedule-deviation weight was zero in the Congestion-Aware mode, the final profile selection was determined by the normalized multi-objective cost among the feasible P4 candidates. This indicates that the selected profile can be affected by the relative spread of the normalized metrics, even when the dominant decision factor is vertiport congestion.

This result suggests that the effective influence of each weight depends not only on the specified weight value, but also on the spread of each normalized metric among feasible candidates.

The system-level delay results further clarify the operational effect of the different vertiport selections. Table 6 compares the observed cumulative ground delay and landing-hold results for the four decision modes.

Table 6. Observed cumulative system-level delay and holding results under 10 m/s wind.

Decision mode	Time-Critical	Schedule-Oriented	Energy-Saving	Congestion-Aware
Ground delay events	8	8	8	7
Landing hold events	2	2	2	0
Cumulative ground delay time [min]	53.92	53.92	53.92	44.33
Cumulative landing hold time [min]	8.75	8.75	8.75	0.0

The Time-Critical, Schedule-Oriented, and Energy-Saving modes ultimately selected Hub2, and these three cases produced the same system-level delay outcome: 53.92 min of cumulative ground delay and 8.75 min of landing-hold time. In contrast, the Congestion-Aware mode maintained P4 throughout the diversion and produced no landing-hold events. This indicates that selecting a less congested vertiport can improve system-level traffic outcomes, even if that option is not the best from the individual aircraft perspective in terms of flight time or battery margin.

The difference in landing-hold time was caused by the interaction between the emergency aircraft and background traffic. In the Hub2 cases, the emergency landing occupied an already congested vertiport and displaced a background aircraft scheduled to land at Hub2, resulting in airborne holding. In contrast, the P4 case produced no landing-hold events. The system-level implications of these vertiport selections are further evaluated against a no-emergency baseline in Section 4.4.

Overall, the 10 m/s wind case demonstrates that the proposed decision framework can reflect different operational priorities when the feasible candidate set is not overly restricted by wind and battery constraints. The Time-Critical and Energy-Saving modes prioritized rapid and energy-efficient landing at Hub2. The Schedule-Oriented mode initially selected a schedule-compatible P4 option but dynamically converged to Hub2 through replanning as schedule error, energy margin, and feasibility

changed. In contrast, the Congestion-Aware mode consistently selected the low-congestion P4 and achieved the most favorable system-level delay outcome. These contrasting behaviors confirm that the proposed framework can adapt the emergency landing decision according to the operational priority expressed by the decision-mode weighting.

4.4 Effect of Decision Mode on System-Level Traffic Delay

To evaluate the system-level impact of the emergency landing decision, a baseline simulation was conducted using the same 23-aircraft traffic scenario, in which the emergency trigger was not activated for the designated emergency aircraft. In this baseline, all 23 aircraft operated according to their pre-planned time-reservation schedules. The cumulative ground delay and landing-hold time observed in the baseline were 46.50 min and 0.00 min, respectively.

Table 7 compares the incremental delay relative to the baseline for each decision mode under the 10 m/s wind condition. The incremental delay is defined as the difference between the cumulative delay observed in each decision-mode simulation and the baseline value.

Table 7. System-level delay comparison relative to baseline under 10 m/s wind.

Decision Mode	Ground Delay [min]	Hold [min]	Incremental Ground Delay [min]	Incremental Hold [min]
Baseline	46.50	0.00	–	–
Time-Critical	53.92	8.75	+7.42	+8.75
Schedule-Oriented	53.92	8.75	+7.42	+8.75
Energy-Saving	53.92	8.75	+7.42	+8.75
Congestion-Aware	44.33	0.00	−2.17	0.00

The Time-Critical, Schedule-Oriented, and Energy-Saving modes all selected Hub2 as the emergency landing destination, resulting in an incremental ground delay of +7.42 min and an incremental landing-hold time of +8.75 min relative to the baseline. These increases were caused by the interaction between the emergency aircraft and background traffic scheduled to use Hub2. Specifically, the emergency landing occupied an already congested vertiport, displacing a background aircraft and inducing airborne holding.

In contrast, the Congestion-Aware mode directed the emergency aircraft to P4, which had no current occupancy or conflicting reservations at the time of the decision. As a result, the cumulative ground delay was 44.33 min, corresponding to an incremental delay of −2.17 min relative to the baseline, and no landing-hold events were observed. The negative incremental ground delay does not imply that the emergency landing improved overall traffic performance. Rather, it reflects that directing the emergency aircraft to the low-congestion P4 avoided additional load on the already-scheduled Hub2 traffic, thereby preventing the airborne holding that occurred in the other three modes.

These results demonstrate that the choice of decision mode has a measurable effect on system-level traffic delay. When the feasible candidate set includes multiple reachable vertiports with different congestion levels, incorporating vertiport congestion into the cost function can mitigate the disruptive impact of emergency landings on surrounding traffic. This finding complements the single-aircraft results presented in Section 4.3 and confirms that the proposed framework can balance individual aircraft safety with system-level operational stability.

5. Conclusion and Future Work

This study proposed a multi-constraint-aware emergency landing decision-support framework for AAM that integrates wind-aware energy estimation, multi-objective candidate evaluation, and periodic replanning. The framework selects among candidate vertiports, guidance strategies, and terminal approach profiles based on arrival time, schedule deviation, energy consumption, and vertiport congestion.

Simulation results demonstrated that periodic replanning enables dynamic guidance strategy switching that cannot be achieved by a static single-point decision. Under the 15 m/s wind condition, the Schedule-Oriented mode initially selected the airspeed-based Strategy B as the only feasible option, then switched to the ground-speed-based Strategy A as the aircraft approached the destination and the required airspeed dropped within the aircraft limit, reducing the schedule error to

zero. This result confirms that the combination of multiple wind-aware guidance strategies and periodic replanning provides robust and schedule-compatible emergency landing decisions under wind disturbances. Under the moderate wind condition, the Congestion-Aware mode further demonstrated that incorporating vertiport congestion into the cost function can reduce system-level holding by directing the emergency aircraft to a less loaded vertiport when multiple reachable options are available.

Future work will address the following issues. First, the wind model should be extended from a constant wind field to a time-varying and spatially varying wind field. Second, the vertiport capacity model should be refined to represent detailed pad, stand, charging, and taxiway constraints rather than using an aggregate capacity value. This would allow the framework to evaluate more realistic vertiport occupancy and turnaround operations. Finally, the decision-support framework should be extended to multiple simultaneous emergency scenarios and operator-in-the-loop evaluations for future m:N AAM operations.

6. Copyright Statement

The authors confirm that they, and/or their company or organization, hold copyright on all of the original material included in this paper. The authors also confirm that they have obtained permission, from the copyright holder of any third party material included in this paper, to publish it as part of their paper. The authors confirm that they give permission, or have obtained permission from the copyright holder of this paper, for the publication and distribution of this paper as part of the ICAS proceedings or as individual off-prints from the proceedings.

References

[1] Federal Aviation Administration, Advanced Air Mobility (AAM) Implementation Plan.

[2] Aubuchon, V. V., Hashemi, K. E., Shively, R. J., and Wishart, J. M., “Multi-Vehicle (m:N) Operations in the NAS – NASA’s Research Plans,” AIAA AVIATION 2022 Forum, Chicago, IL, USA, 2022. doi: 10.2514/6.2022-3758.

[3] Pradeep, P., Kulkarni, C. S., Chatterji, G. B., and Lauderdale, T. A., “Parametric Study of State-of-Charge for an Electric Aircraft in Urban Air Mobility,” AIAA AVIATION 2021 Forum, 2021. doi: 10.2514/6.2021-3181.

[4] Song, K., and Yeo, H., “Development of Optimal Scheduling Strategy and Approach Control Model of Multicopter VTOL Aircraft for Urban Air Mobility (UAM) Operation,” Transportation Research Part C: Emerging Technologies, Vol. 128, 103181, 2021. doi: 10.1016/j.trc.2021.103181.

[5] Fang, X., Jiang, J., and Chen, W.-H., “Model Predictive Approach for Wind-Aware Forced Landing,” IEEE Transactions on Aerospace and Electronic Systems, Vol. 59, pp. 3995–4004, 2023. doi: 10.1109/TAES.2023.3235321.

[6] Ma, L., Ding, Y., and Yang, J., "Autonomous Emergency Gliding Landing Guidance and Control of Tilt-Wing Electric Vertical Take-Off and Landing for Urban Air Mobility Missions Using Control Barrier Functions," Aerospace, Vol. 12, No. 1, Article 63, 2025. doi: 10.3390/aerospace12010063.

[7] Schweiger, K., Schmitz, R., and Knabe, F., "Impact of Wind on eVTOL Operations and Implications for Vertiport Airside Traffic Flows: A Case Study of Hamburg and Munich," Drones, Vol. 7, No. 7, Article 464, 2023. doi: 10.3390/drones7070464.